POLITECNICO MILANO 1863

SCUOLA DI INGEGNERIA INDUSTRIALE E DELL'INFORMAZIONE

Executive Summary of the Thesis

Predictor-Based Adaptive Control and Allocation for multirotor UAVs

Laurea Magistrale in Aeronautical Engineering - Ingegneria Aeronautica

Author: Nicolò Borsa

Advisor: Prof. Davide Invernizzi

Co-advisor: Giovanni Gozzini

Academic year: 2024-2025

1. Introduction

Autonomous aerial vehicles are increasingly deployed in safety-critical, high-precision missions, both in commercial (delivery, media production) and non-commercial contexts (humanitarian, agricultural, military). These applications impose stringent requirements on reliability, precision, and robustness.
Conventional control architectures perform well only under nominal conditions and may degrade significantly in the presence of modeling uncertainties, external disturbances, and actuator faults, possibly leading to instability.
Therefore, the adoption of adaptive and fault-tolerant control strategies is necessary to guarantee acceptable performance under non-nominal operating conditions.

Autonomous aerial vehicles are highly sensitive to modeling uncertainties, wind disturbances, and actuator faults, which can significantly degrade performance or even compromise stability under non-nominal conditions.
To address these challenges, this work proposes an augmented adaptive control framework for a quadrotor that integrates Predictor-based Model Reference Adaptive Control (P-MRAC) with control allocation [1, 2]. The approach enables online compensation of uncertainties, disturbances, and actuator degradation while reducing the number of adaptive parameters and improving real-time implementability.
The objective is to enhance robustness and fault tolerance while maintaining high performance in the presence of non-ideal operating conditions.

The main contributions of this work are an augmented adaptive controller design developed in a modular way, where the quadrotor attitude and position subsystems are adaptively augmented independently and then coordinated through an adaptive control allocation layer. To keep the adaptive augmentation lightweight and well-conditioned, the approach reduces the number of parameters using an SVD-based projection onto an input subspace. Finally, the framework is validated experimentally in the presence of actuator degradation and wind disturbances.

2. Augmented P-MRAC approach with parameter reduction due to overactuation

2.1. Uncertain dynamical model

The following representation of an uncertain dynamical system, in which the rigid-body dynamics is separated from the actuator dynamics, is considered:

$$\begin{aligned} \dot{x}_p(t) &= A_p x_p + B_\nu(\nu_{act}(t) + \varphi(x_p(t), t)\theta_p) + d \\ \nu_{act}(t) &= B_a \Lambda \,\mathrm{sat}(u_{act}(t)) \end{aligned} \tag{1}$$

2.2. Predictor Model

A state predictor is used to estimate the plant state $x_p(t)$ and the unknown parameters.
It is defined as:

$$\begin{aligned} \dot{\hat{x}}_p(t) &= A_p \hat{x}_p + B_\nu \hat{\nu}(t) + B_\nu(\hat{\nu}_{act}(t) - \hat{\nu}(t)) \\ &\quad + L(x_p - \hat{x}_p) + B_\nu \varphi \hat{\theta}_p \\ \hat{\nu}(t) &= \hat{\nu}_{bl} + \hat{\nu}_{aug} = B_a \hat{\Lambda} u(t) \\ \hat{\nu}_{act}(t) &= \hat{\nu}_{bl,act} + \hat{\nu}_{aug,act} = B_a \hat{\Lambda}\,\mathrm{sat}(u_{act}(t)) \\ \hat{\nu}_{aug} &= -\varphi \hat{\theta}_p \end{aligned} \tag{2}$$

2.3. Singular Value Decomposition of the Input Map

A Singular Value Decomposition (SVD) on the matrix B_a is performed:

$$B_a = U_a \Sigma_a V_a^\top \tag{3}$$

where $\Sigma_a \in R^{r\times m}$ is a rectangular matrix with non-negative singular values on the diagonal, $U_a \in R^{r\times r}$ and $V_a \in R^{m\times m}$ are orthogonal matrices.
If the system is overactuated, a modification can be made to the singular value decomposition (SVD) of B_a.

$$B_a = U_{ar} D_a V_{ar}^\top \tag{4}$$

where U_{ar}, D_a, and V_{ar}, are the non-null part of U_a, Σ_a, and V_a respectively.
Therefore, the second equation of (2), can be rewritten as:

$$\hat{\nu}(t) = U_{ar} D_a V_{ar}^\top \hat{\Lambda} u(t) = U_{ar} D_a \hat{\Lambda}_{ar} u(t) \tag{5}$$

Furthermore, instead of estimating Λ_{ar}, $\Lambda_{aa} = V_{ar}^\top \Lambda V_a$ is considered. This formulation allows to further reduce the number of parameters (if Λ is assumed as a full matrix) to be estimated and guarantees the positive definiteness of the Lyapunov candidate function, later employed in the derivation of the update laws.

2.4. Update Laws with parameter reduction thanks to overactuation

Next step is the derivation of the appropriate update laws for the parameters $\hat{\theta}_p$ and $\hat{\Lambda}_{aa}$.
From (1) and (2), and by defining:

$$\begin{aligned} \tilde{\nu}_{act} &= \nu_{act} - \hat{\nu}_{act} = B_a(\Lambda - \hat{\Lambda})\,\mathrm{sat}(u_{act}) \\ &= U_{ar} D_a V_{ar}^\top \tilde{\Lambda} V_a V_a^\top \,\mathrm{sat}(u_{act}) \\ &= U_{ar} D_a \tilde{\Lambda}_{aa} V_a^\top \,\mathrm{sat}(u_{act}) \\ \tilde{\theta}_p &= \theta_p - \hat{\theta}_p \end{aligned} \tag{6}$$

The predictor error dynamics can be computed as:

$$\begin{aligned} \dot{e}_p &= (A_p - L)e_p + B_\nu \tilde{\nu}_{act} + B_\nu \varphi \tilde{\theta}_p \\ &= (A_p - L)e_p + B_\nu U_{ar} D_a \tilde{\Lambda}_{aa} V_a^\top \,\mathrm{sat}(u_{act}) \\ &\quad + B_\nu \varphi \tilde{\theta}_p \end{aligned} \tag{7}$$

The update laws for the parameters $\dot{\hat{\theta}}_p$ and $\dot{\hat{\Lambda}}_{aa}$, derived from Lyapunov stability analysis, assume this form:

$$\begin{aligned} \dot{\hat{\theta}}_p &= \Gamma_\theta \varphi^\top B_\nu^\top e_p \\ \dot{\hat{\Lambda}}_{aa} &= \Gamma_\Lambda D_a U_{ar}^\top B_\nu^\top e_p \,\mathrm{sat}(u_{act})^\top V_a, \end{aligned} \tag{8}$$

and such that $\hat{\Lambda}_{ar} = \hat{\Lambda}_{aa} V_a^\top$.

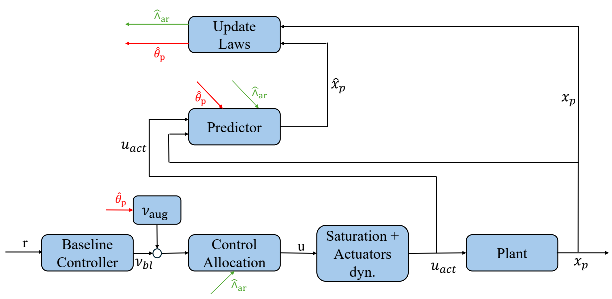

Figure 1: Augmented P-MRAC structure.

2.5. Update Laws without reduction

Alternatively, by assuming the control effectiveness matrix Λ to be diagonal rather than a full matrix, its structural properties can be exploited to derive a dedicated update law directly for $\hat{\Lambda}$, instead of for the projected matrix $\hat{\Lambda}_{aa}$. In particular, it is possible to estimate only the elements on the diagonal, due to the fact that the

other elements are equal to 0.
The virtual controls error is newly defined as:

$$\begin{aligned}\tilde{\nu}_{act} &= \nu_{act} - \hat{\nu}_{act} = B_a(\Lambda - \hat{\Lambda})\,\mathrm{sat}(u_{act}) \\ &= B_a\,\mathrm{diag}(\mathrm{sat}(u_{act}))\tilde{\lambda} = B_a U_{\mathrm{diag}}\tilde{\lambda}\end{aligned} \tag{9}$$

The predictor error dynamic can be rewritten as:

$$\dot{e}_p = (A_p - L)e_p + B_\nu B_a U_{\mathrm{diag}}\tilde{\lambda} + B_\nu \varphi \tilde{\theta}_p \tag{10}$$

The update laws for the new parameters $\dot{\hat{\theta}}_p$ and $\dot{\hat{\lambda}}$, still derived from Lyapunov stability analysis, assume this form:

$$\begin{aligned}\dot{\hat{\theta}}_p &= \Gamma_\theta \varphi^\top B_\nu^\top e_p \\ \dot{\hat{\lambda}} &= \Gamma_\lambda U_{\mathrm{diag}}^\top B_a^\top B_\nu^\top e_p \rightarrow \hat{\Lambda} = \mathrm{diag}(\hat{\lambda})\end{aligned} \tag{11}$$

Remark. Due to the possible presence of noise or unmodeled disturbances during the simulations, some robust modifications need to be made to the update laws. In particular, an upper and lower saturation limit is considered on the values of the parameter $\hat{\Lambda}_{aa}$ (or $\hat{\lambda}$), and a Projection Operator is applied to $\hat{\theta}_p$.

3. Adaptive augmentation and allocation strategies for vector-thrust UAVs

In this chapter, the Augmented P-MRAC approach is applied the class of vector-thrust quadrotor UAVs.

3.1. Control-Oriented Model

Attitude dynamics and kinematic, expressed in the body frame, and Position dynamics and kinematics, expressed in the inertial frame, for a generic vector-thrust quadrotor UAV, are the following:

$$\begin{cases} J\dot{\omega}_b = -\omega_b^\times J\omega_b - D_{\tau\omega}\omega_b + \tau_c + d_\tau \\ \dot{R} = R\omega_b^\times \\ m\dot{v}_i = mge_3 - RD_{fv}R^\top v_i - T_c Re_3 + d_f \\ \dot{p} = v_i \end{cases} \tag{12}$$

Defining $u = (T_1, T_2, T_3, T_4)_{cmd}$, so having as control inputs the thrusts provided by each propeller, a simple linear mapping (using B_a = input map) of the thrust generated by each propeller with the virtual control inputs, can be derived:

$$\begin{bmatrix} 0 \\ 0 \\ T_c \\ \ell_c \\ m_c \\ n_c \end{bmatrix} = B_a \begin{bmatrix} T_1 \\ T_2 \\ T_3 \\ T_4 \end{bmatrix} = \begin{bmatrix} W_{Tc} \\ W_M \end{bmatrix} \begin{bmatrix} T_1 \\ T_2 \\ T_3 \\ T_4 \end{bmatrix} \tag{13}$$

3.2. Trajectory tracking control problem and baseline control system

Control problem is solved by a two-level control architecture, made by a high level motion controller, and an allocation algorithm.
A hierarchical control framework is proposed in which position and attitude are controlled separately. In particular the outer controller will be the position controller, while the inner one will be the attitude controller.
Position Controller: The virtual control force f_c is selected using this simple P/PI structure:

$$\begin{aligned}\dot{x}_{iv} &= v_i - v_c \\ f_c &= \sigma_{mf}(-K_v(v_i - v_c) - K_{iv}x_{iv} + m(\dot{v}_c - ge_3)).\end{aligned}$$

where the velocity command is selected using a proportional controller:

$$v_C = -\sigma_{mv}(K_p(p - p_d)) + v_d \tag{14}$$

Attitude Controller: the inner loop attitude controller is given by a P/PI law:

$$\begin{aligned}\dot{x}_{i\omega} &= \omega_e \\ \tau_c &= -K_\omega \omega_e - K_{i\omega}x_{i\omega} + \omega_c^\times J\omega_b + J\dot{\omega}_c\end{aligned} \tag{15}$$

3.3. Augmented P-MRAC controller architectures

Given the generic vector-thrust quadrotor UAV model introduced above, two different Augmented P-MRAC architectures are considered and analyzed:

1. A single augmented controller is employed, in which the attitude and position dynamics are combined into a unified dynamical model.
2. The Augmented P-MRAC framework is applied separately to the attitude and position dynamics subsystems.

3.4. Augmented P-MRAC approach on the full uncertain vector-thrust quadrotor UAV

This section presents the first architecture of the Augmented P-MRAC approach applied to the full vector-thrust quadrotor UAV.
In particular, a single augmented controller is employed. In this case, the attitude and position dynamics are combined into a unified model, and a single predictor is used.
The unified model, can be written as follows:

$$\begin{aligned}\dot{x}_p &= A_p x_p + B_\nu \nu_{act} + B_\nu \varphi_x \theta_{Ap} + d \\ &\quad + \begin{bmatrix} gRk_b & -J^{-1}\omega_b^\times J\omega_b \end{bmatrix}^\top \\ x_p &= \begin{bmatrix} v_x & v_y & v_z & p & q & r \end{bmatrix}^\top \\ A_p &= \begin{bmatrix} -\frac{D_{fv}}{m} & 0 \\ 0 & -J^{-1}D_{\tau\omega} \end{bmatrix} \\ B_\nu &= \begin{bmatrix} -\frac{I}{m} & 0 \\ 0 & J^{-1} \end{bmatrix} \\ \nu_{act} &= B_a \Lambda \,\mathrm{sat}(u_{act})\end{aligned} \tag{16}$$

A predictor model analogous to (2) can then be defined as:

$$\begin{aligned}\dot{\hat{x}}_b &= A_p \hat{x}_b + B_\nu \hat{\nu} + B_\nu(\hat{\nu}_{act} - \hat{\nu}) \\ &\quad + L(x_b - \hat{x}_b) + B_\nu \varphi_x \hat{\theta}_{Ap} + B_\nu \varphi_d \hat{\theta}_d \\ &\quad + \begin{bmatrix} gRk_b & -J^{-1}\omega_b^\times J\omega_b \end{bmatrix}^\top \\ \hat{\nu}(t) &= \hat{\nu}_{bl} + \hat{\nu}_{aug} = B_a \hat{\Lambda}\,\mathrm{sat}(u_{act}) \\ \hat{\nu}_{aug} &= -(\varphi_x \hat{\theta}_{Ap} + \varphi_d \hat{\theta}_d)\end{aligned} \tag{17}$$

It can be observed that uncertainties affecting the system matrix A_p and input disturbances are treated separately by introducing two distinct regressor functions and parameter vectors. In particular, φ_x depends solely on the system state x_b, while φ_d is defined as a function of a unitary vector.
Proceeding as in Section (2.5), the following parameters update laws are obtained:

$$\begin{aligned}\dot{\hat{\theta}}_{Ap} &= \Gamma_{\theta_{Ap}} \varphi_x^\top B_\nu^\top e_p \\ \dot{\hat{\theta}}_d &= \Gamma_{\theta_d} \varphi_d^\top B_\nu^\top e_p \\ \dot{\hat{\lambda}} &= \Gamma_\lambda U_{\mathrm{diag}} B_a^\top B_\nu^\top e_p \to \dot{\hat{\Lambda}} = \mathrm{diag}(\dot{\hat{\lambda}})\end{aligned} \tag{18}$$

The adaptive control allocation algorithm implemented is the following.
Exploiting the properties of the diagonal matrices, the inverse of $\hat{\Lambda}$ can be easily found by:

$$\begin{aligned}\hat{\lambda} &= \begin{bmatrix} \hat{\lambda}_1 & \hat{\lambda}_2 & \hat{\lambda}_3 & \hat{\lambda}_4 \end{bmatrix}^\top \\ \hat{\Lambda}^{-1} &= \mathrm{diag}\left(\begin{bmatrix} \frac{1}{\hat{\lambda}_1} & \frac{1}{\hat{\lambda}_2} & \frac{1}{\hat{\lambda}_3} & \frac{1}{\hat{\lambda}_4} \end{bmatrix}^\top \right) \\ \hat{\lambda}_i &= 0 \to \frac{1}{\hat{\lambda}_i} \approx 0\end{aligned} \tag{19}$$

Finally, the adaptive control allocation law is obtained as:

$$u(t) = \hat{\Lambda}^{-1}\,\mathrm{pinv}(B_a)\nu(t) \tag{20}$$

where, $\mathrm{pinv}(B_a)$ is computed offline.

3.5. Augmented P-MRAC approach for the uncertain attitude subsystem

The attitude dynamic equation can be written in this way:

$$\begin{aligned}\dot{\omega}_b &= -J^{-1}D_{\tau\omega}\omega_b + J^{-1}\tau_c \\ &\quad - J^{-1}\omega_b^\times J\omega_b + J^{-1}d_\tau \\ \tau_c &= W_M \Lambda\,\mathrm{sat}(u_{act}) \\ A_{p,att} &= -J^{-1}D_{\tau\omega} \\ B_{\nu,att} &= J^{-1}.\end{aligned}$$

Exploiting the overactuation of W_M, the attitude predictor model can be derived as:

$$\begin{aligned}\dot{\hat{\omega}}_b &= A_{p,att}\hat{\omega}_b + B_{\nu,att} U_{Mr} D_M \hat{\Lambda}_{Mr} u(t) \\ &\quad + B_{\nu,att} U_{Mr} D_M \hat{\Lambda}_{Mr}(\mathrm{sat}(u_{act}(t)) - u(t)) \\ &\quad - J^{-1}\hat{\omega}_b^\times J\hat{\omega}_b + L(\omega_b - \hat{\omega}_b) \\ &\quad + B_{\nu,att}\varphi_x \hat{\theta}_{Ap} + B_{\nu,att}\varphi_d \hat{\theta}_d \\ \hat{\nu}(t) &= \hat{\nu}_{bl} + \hat{\nu}_{aug} = W_M \hat{\Lambda}\,\mathrm{sat}(u_{act}) \\ &= U_{Mr} D_M \hat{\Lambda}_{Mr}\,\mathrm{sat}(u_{act}) \\ \hat{\nu}_{aug} &= -(\varphi_x \hat{\theta}_{Ap} + \varphi_d \hat{\theta}_d)\end{aligned}$$

with the following update laws:

$$\begin{aligned}\dot{\hat{\theta}}_{Ap} &= \Gamma_{\theta_{Ap},att} \varphi_x^\top B_{\nu,att}^\top e_\omega \\ \dot{\hat{\theta}}_d &= \Gamma_{\theta_d,att} \varphi_d^\top B_{\nu,att}^\top e_\omega \\ \dot{\hat{\Lambda}}_{MM} &= \Gamma_{\Lambda,att} D_M^\top U_{Mr}^\top B_{\nu,att}^\top e_\omega\,\mathrm{sat}(u_{act})^\top V_M \\ \dot{\hat{\Lambda}}_{Mr} &= \dot{\hat{\Lambda}}_{MM} \cdot V_M^\top\end{aligned}$$

For a quadrotor drone, it is possible to exploit the structure of the control effectiveness matrix

Λ_{MM}, to reduce the number of parameters required for its estimation by leveraging system symmetries.
The generic Λ_{MM}, it can be written as:

$$\Lambda_{MM} = \begin{bmatrix} \lambda_{MM_1} & \lambda_{MM_2} & \lambda_{MM_3} & \lambda_{MM_4} \\ \lambda_{MM_2} & \lambda_{MM_1} & \lambda_{MM_4} & \lambda_{MM_3} \\ \lambda_{MM_3} & \lambda_{MM_4} & \lambda_{MM_1} & \lambda_{MM_2} \end{bmatrix} \tag{21}$$

Therefore, a reduction of the number of parameters of $V_{Mr}^\top \dot{\hat{\Lambda}} V_M$ needed to be estimates from twelve to four is possible.
Recalling the previous equation, it can be alternatively rewritten as:

$$\lambda_{MM} = \begin{bmatrix} \lambda_{MM_1} \\ \lambda_{MM_2} \\ \lambda_{MM_3} \\ \lambda_{MM_4} \end{bmatrix} = B_\Lambda \cdot \begin{bmatrix} \lambda_1 \\ \lambda_2 \\ \lambda_3 \\ \lambda_4 \end{bmatrix} = B_\Lambda \lambda \tag{22}$$

Considering the equation (22), the equation (10), applied to the attitude dynamics, can be rewritten as:

$$\begin{aligned} \dot{e}_\omega &= (A_{p,att} - L_{att}) e_\omega \\ &+ B_{\nu,att} W_M U_{\text{diag}} B_\Lambda^{-1} \tilde{\lambda}_{MM} \\ &+ B_{\nu,att} \varphi_x \tilde{\theta}_{Ap} + B_{\nu,att} \varphi_d \tilde{\theta}_d. \end{aligned} \tag{23}$$

Then, the following update laws can be derived:

$$\begin{aligned} \dot{\hat{\theta}}_{Ap} &= \Gamma_{\theta_{Ap},att} \varphi_x^\top B_{\nu,att}^\top e_\omega \\ \dot{\hat{\theta}}_d &= \Gamma_{\theta_{d},att} \varphi_d^\top B_{\nu,att}^\top e_\omega \\ \dot{\hat{\lambda}}_{MM} &= \Gamma_{\Lambda,att} {B_\Lambda^{-1}}^\top U_{\text{diag}}^\top W_M^\top B_{\nu,att}^\top e_\omega \\ \dot{\hat{\Lambda}}_{MM} &= \begin{bmatrix} \dot{\hat{\lambda}}_{MM_1} & \dot{\hat{\lambda}}_{MM_2} & \dot{\hat{\lambda}}_{MM_3} & \dot{\hat{\lambda}}_{MM_4} \\ \dot{\hat{\lambda}}_{MM_2} & \dot{\hat{\lambda}}_{MM_1} & \dot{\hat{\lambda}}_{MM_4} & \dot{\hat{\lambda}}_{MM_3} \\ \dot{\hat{\lambda}}_{MM_3} & \dot{\hat{\lambda}}_{MM_4} & \dot{\hat{\lambda}}_{MM_1} & \dot{\hat{\lambda}}_{MM_2} \end{bmatrix} \end{aligned} \tag{24}$$

3.6. Augmented P-MRAC approach for the uncertain position subsystem

The position dynamics equation can be written, in the body frame to lose its time dependence, in this way:

$$\begin{aligned} \dot{v}_b &= -\frac{D_{fv}}{m} v_b - \frac{I}{m} T_{cv} + gRk_b + \frac{d_T}{m} \\ T_{cv} &= \begin{bmatrix} 0 \\ 0 \\ T_c \end{bmatrix} = W_{Tc} \Lambda \operatorname{sat}(u_{act}) \end{aligned} \tag{25}$$

$$\begin{aligned} A_{p,pos} &= -\frac{D_{fv}}{m} \\ B_{\nu,pos} &= -\frac{I}{m} = \begin{bmatrix} -\frac{1}{m} & 0 & 0 \\ 0 & -\frac{1}{m} & 0 \\ 0 & 0 & -\frac{1}{m} \end{bmatrix} \end{aligned} \tag{26}$$

The position predictor model is derived as:

$$\begin{aligned} \dot{\hat{v}}_b &= A_{p,pos} \hat{v}_b + B_{\nu,pos} \hat{T}_{cv} \\ &+ B_{\nu,pos} (\hat{T}_{cv,act} - \hat{T}_{cv}) + L(v_b - \hat{v}_b) \\ &+ B_{\nu,pos} \varphi_d \hat{\theta}_d + B_{\nu,pos} \varphi_x \hat{\theta}_{Ap} + gRk_b \\ \hat{T}_{cv}(t) &= \hat{T}_{cv,bl} + \hat{T}_{cv,aug} = W_{Tc} \Lambda \operatorname{sat}(u_{act}) \\ &= U_{Tr} D_T \hat{\Lambda}_{Tr} \operatorname{sat}(u_{act}) \\ \hat{T}_{cv,aug} &= -(\varphi_d \hat{\theta}_d + \varphi_x \hat{\theta}_{Ap}) \end{aligned}$$

with the following update laws:

$$\begin{aligned} \dot{\hat{\theta}}_d &= \Gamma_{\theta_d,pos} \varphi_d^\top B_{\nu,pos}^\top e_v \\ \dot{\hat{\theta}}_{Ap} &= \Gamma_{\theta_{Ap},pos} \varphi_x^\top B_{\nu,pos}^\top e_v \\ \dot{\hat{\Lambda}}_{TT} &= \Gamma_{\Lambda,pos} D_T U_{Tr}^\top B_{\nu,pos}^\top e_v \operatorname{sat}(u_{act})^\top V_T \end{aligned}$$

3.7. Combined attitude-position Augmented P-MRAC using Adaptive Control Allocation

The two previous Augmented P-MRAC controllers are applied to their respective baseline controllers, exploiting the hierarchical control framework of the full vector-thrust quadrotor UAV (second architecture of (3.3)).
The Adaptive Control Allocation strategy adopted in this case is the following.
With the knowledge of $\hat{\Lambda}_{MM}$ and $\hat{\Lambda}_{TT}$, it is possible to reconstruct $\hat{\Lambda}$.
However, a full 4×4 control effectiveness matrix $\hat{\Lambda}$ is estimated, with this structure:

$$\hat{\Lambda} = \begin{bmatrix} \lambda_1 & b & c & d \\ a & \lambda_2 & c & d \\ a & b & \lambda_3 & d \\ a & b & c & \lambda_4 \end{bmatrix} \tag{27}$$

Considering the Sherman-Morrison theorem, by selecting r, v and D in this way;

$$\begin{aligned} r &= \begin{bmatrix} 1 & 1 & 1 & 1 \end{bmatrix}^\top \\ v &= \begin{bmatrix} a & b & c & d \end{bmatrix}^\top \\ D &= \hat{\Lambda} - rv^\top \end{aligned} \tag{28}$$

and, due to the fact that D is always a diagonal matrix, if $(1 + v^\top D^{-1} r) \neq 0$, the inverse of $\hat{\Lambda}$, can be computed in this way:

$$\hat{\Lambda}^{-1} = (D + rv^\top)^{-1} = D^{-1} - \frac{D^{-1} r v^\top D^{-1}}{1 + v^\top D^{-1} r}$$

Only products between matrices and vectors are needed, which need less computational power and are easier to implement in real-time systems. After this, a real-time adaptive control allocation algorithm can be applied:

$$
\begin{aligned}
u(t) &= \hat{\Lambda}^{-1}\,\mathrm{pinv}(B_a)\nu(t) \\
&= (D + rv^\top)^{-1}\,\mathrm{pinv}(B_a)\nu(t) \\
&= \left(D^{-1} - \frac{D^{-1}rv^\top D^{-1}}{1 + v^\top D^{-1} r}\right)\mathrm{pinv}(B_a)\nu(t)
\end{aligned}
$$

where D^{-1} is computed as (19). Since B_a is known and constant, $\mathrm{pinv}(B_a)$ can be computed offline

4. Experimental results

After numerical simulations that show better overall performance of the second architecture proposed in Section 3.7, compared to the first one proposed in Section 3.4, experimental validation on a physical ANT-X quadrotor drone has been carried out. Only the second version (the divided formulation) of the Augmented P-MRAC controller has been implemented on the physical platform.

In the first two real-world experiments, only actuator efficiency degradations were introduced. In the first experiment, a uniform degradation was applied to all rotors. In the second experiment, a more severe degradation was applied specifically to the third rotor, both in the absence of external disturbances. The experimental results demonstrated a significant improvement in performance and stability when the adaptive controller was enabled, compared to the behavior obtained using only the baseline controller.

In the second experiment, a degradation of 20% of the third rotor plus a constant external wind disturbance along the East direction in hoovering condition is considered.
By analyzing the position time histories in Figure 4, an initial peak caused by the external disturbance can be observed along the East direction and in altitude. Subsequently, further peaks appear in all position components due to the rotor fault. By comparing the two response, the baseline controller (Figure 4b) exhibits peaks which are approximately 2/3 times larger than the adaptive controller (Figure 4a).
By analyzing the Figure 2, the estimation accuracy of the diagonal elements of $\hat{\Lambda}(t)$ can be considered high, as the true efficiency reduction is reconstructed almost exactly.

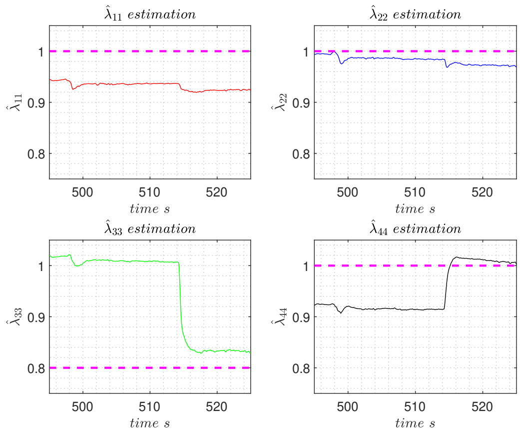

Figure 2: Estimated effectiveness $\hat{\Lambda}$ with a fault on the third rotor.

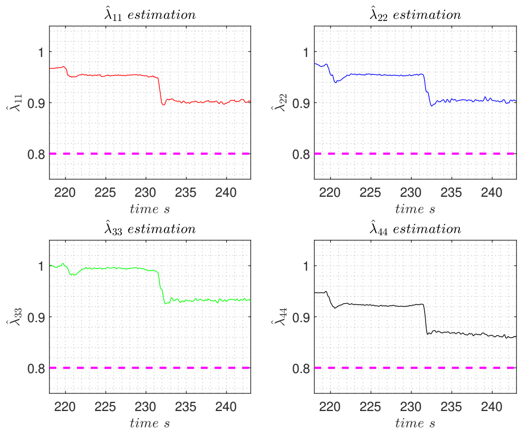

Figure 3: Estimated effectiveness $\hat{\Lambda}$ with a fault on all rotors and wind disturbance.

In the third experiment a degradation of 20% of all rotors plus an higher external wind disturbances along the East direction while the drone is in hover is considered.
By analyzing the position time histories in Figure 5, it is evident that also under these conditions the transient required to restore hovering conditions after the fault or after the start of the wind disturbance is noticeably shorter in the adaptive case. This clearly highlights the benefit of the adaptive augmentation in compensating for actuator efficiency losses.
By analyzing the Figure 3, it can be stated that the estimation accuracy of $\hat{\Lambda}(t)$ can be considered satisfactory, as the efficiency reduction is reconstructed with good accuracy.

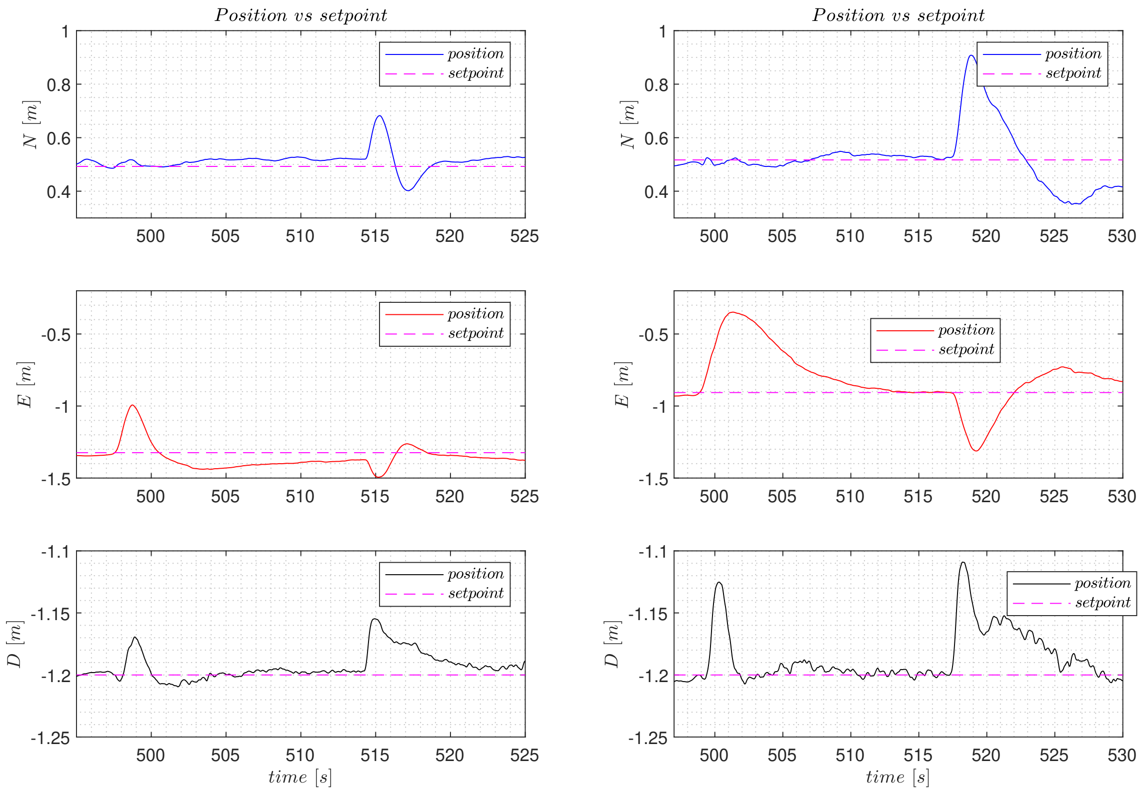

(a) Position Augmented. (b) Position Baseline.

Figure 4: North, East and Down position with fault on the third rotor and constant wind disturbance in the East direction.

As can be observed, the overall estimation accuracy is poorer than in the case where the fault affects only the third rotor. This difference is attributable to the nature of the fault. In particular, a uniform efficiency reduction across all rotors can be effectively compensated for, and equivalently modeled as, a constant disturbance acting along the vertical axis. This interpretation is further supported by the estimated external disturbance terms. By comparing the vertical disturbance estimates in Figure 6 and Figure 7, it can be observed that the vertical component is larger in the former case. This indicates that the efficiency degradation is primarily compensated through the estimation of an equivalent external force acting in the vertical direction.

5. Conclusions

Based on the analyses presented throughout this thesis, the effectiveness and benefits of applying an Augmented P-MRAC adaptive controller to a quadrotor drone, are clearly demonstrated. In particular, real-world experimental results, supported by comparisons with both baseline controller performance and simulation outcomes, confirm that the Augmented P-MRAC controller performs effectively in real-life operating conditions, achieving a substantial improvement in robustness and tracking performance.

References

[1] D. Invernizzi and A. Serrani. Predictor-based adaptive plant augmentation design with application to hierarchical control. *IEEE Control Systems Letters*, 8:502–507, 2024.

[2] G. P. Falconí Salazar. *Adaptive Fault Tolerant Control for VTOL Aircraft with Actuator Redundancy*. PhD thesis, Technical University of Munich, 2022.

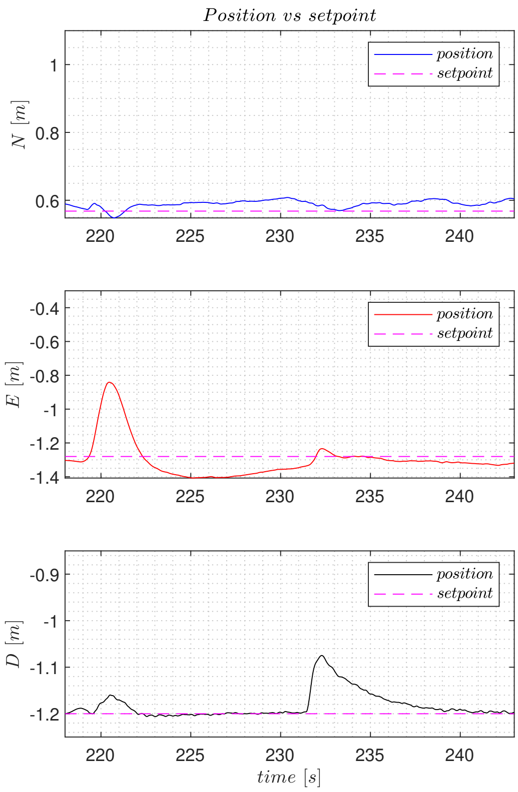

(a) Position Adaptive.

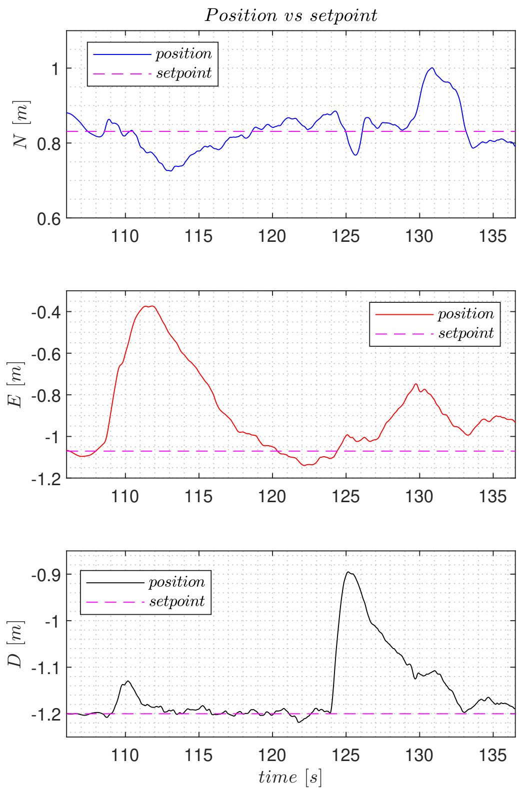

(b) Position Baseline.

Figure 5: North, East and Down position with fault on all the rotors and constant wind disturbance in the East direction.

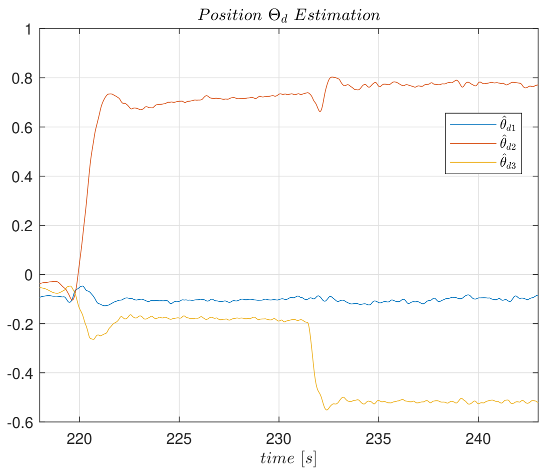

Figure 6: Estimated disturbance $\hat{\theta}_{d_{pos}}(t)$ for the experiment with external wind disturbance and degradation of all rotors.

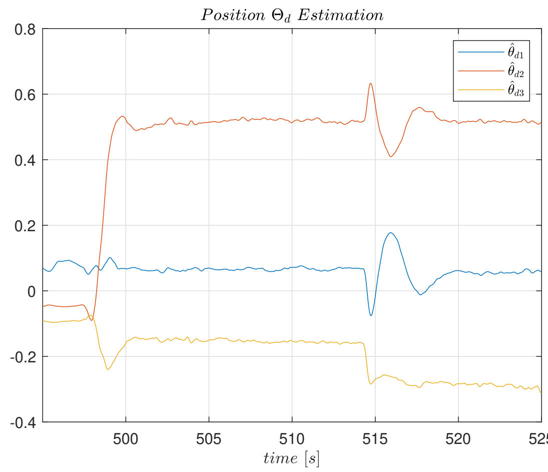

Figure 7: Estimated disturbances $\hat{\theta}_{d_{pos}}(t)$ for the experiment with external wind disturbance and degradation of the third rotor.